

Point Cloud Semantic Segmentation using Multi Scale Sparse Convolution Neural Network

Yunzheng Su

School of Optics and Photonics
Beijing Institution of Technology
BeiJing 100081, China
suyunzzz@bit.edu.cn

Lei Jiang

School of Optics and Photonics
Beijing Institution of Technology
BeiJing 100081, China
fabulousJerry@163.com

May 24, 2022

Abstract

In recent years, with the development of computing resources and LiDAR, point cloud semantic segmentation has attracted many researchers. For the sparsity of point clouds, although there is already a way to deal with sparse convolution, multi-scale features are not considered. In this letter, we propose a feature extraction module based on multi-scale sparse convolution and a feature selection module based on channel attention and build a point cloud segmentation network framework based on this. By introducing multi-scale sparse convolution, the network could capture richer feature information based on convolution kernels with different sizes, improving the segmentation result of point cloud segmentation. Experimental results on Stanford large-scale 3-D Indoor Spaces(S3DIS) dataset and outdoor dataset(SemanticKITTI), demonstrate effectiveness and superiority of the proposed method.

1 Introduction

With the development of stereo matching algorithms and 3D sensors, the importance of point cloud data has become increasingly prominent. The point cloud data contains the three-dimensional coordinates, color, intensity and other information of the scene, which can naturally describe the natural scene. Compared with the two-dimensional image, although the point cloud cannot describe the texture information of the target surface, the three-dimensional point cloud can

directly obtain the distance information of the target, which is more in line with our common sense of life. High-quality point cloud data is the bridge between the virtual world and the real world, Through the processing of point cloud data, environmental information can be better perceived, and semantics can enrich the information conveyed by the point cloud. This is of great significance for research directions such as computer vision, intelligent driving, remote sensing mapping, and smart cities.

Point cloud segmentation can precisely determine the shape, category, and other properties of objects of interest in the scene. Taking intelligent driving as an example, as an upstream module, point cloud semantic segmentation needs to segment the ground elements, road signs, and other information based on the point cloud data obtained, to determine the position of the vehicle in combination with the high-definition(HD) maps or perform LiDAR detection([1, 2, 3, 4, 5]). HD maps are a combination of 3D point clouds and relevant semantic information. In the production of HD maps, it is necessary to segment the point cloud map collected by the onboard sensor and then vectorize map elements.

By analogy with 2D image semantic segmentation, point cloud semantic segmentation and 2D image semantic segmentation are similar in definition and are both fine-grained classification of data. Different from 2D images, point clouds are unstructured and have uneven density distribution at different distances. These characteristics make point cloud semantic segmentation more difficult than images. Nevertheless, research in point cloud semantic segmentation has seen an increase in the past few years, a series of point cloud semantic segmentation datasets have emerged, such as semanticKITTI[6]

Unstructured properties and sparsity bring challenges to point cloud semantic segmentation. However, there are many successful methods have been proposed in the literature². For the unstructured nature of point clouds, thanks to the excellent performance of convolutional neural networks in image processing, one of the solutions is to extract features from point clouds based on two-dimensional convolutional neural networks. Through the projection operation, the three-dimensional information can be converted to two-dimensional and then processed by the two-dimensional convolutional neural network, and finally, the result is back-projected to the three-dimensional. In the process of projecting and back-projection, it will cause some information loss inevitably and introduce inconsistency in the back-projection stage. Another solution is to divide the point cloud into voxels, and then use a 3D convolutional neural network to extract features from the point cloud. While these methods maintain the original features of the point cloud, the performance and efficiency depend on the voxel-resolution, so it is inevitable to make a trade-off between performance and time-consuming. For the sparsity of point clouds, sparse voxel-based methods reduce computing resource usage and improve efficiency by reducing memory usage and computing performance cost on empty voxel in point cloud, but only single-scale features can be obtained. To better process point cloud in 3D and to take advantage of sparsity, we proposed MSSNet, which is built upon MinkowskiEngine[7] and uses multi-scale sparse convolution kernel to extract features with different scales, We summarize the main contributions as:

-
- We proposed a novel multi-scale feature extraction and fusion module based on sparse convolution called MFFM, which extract multi scale feature and adaptively selective fusion by select kernel attention mechanism.
 - We proposed an attention-based feature filter module to avoid the problem of introducing redundant features by multi-scale feature, and construct a high performance network called MSSNet based on our multi-scale feature fusion module and feature filter module. The network can be used for indoor point cloud semantic segmentation as well as outdoors with low-latency.
 - We conducted extensive experiments and analysis on benchmark datasets and compare with previous methods, our method achieves leading results

2 Related Work

2.1 Point-based method

PointNet[8] proposes to use a shared multilayer perceptron to learn point-wise features, and use a symmetric function to learn the global features of the point cloud. The proposed architecture successfully extracts the point-wise feature from irregular and unordered point set. Inspired by PointNet, a series of point-based networks are proposed. Aiming at the problem that PointNet can only learn features point by point and cannot obtain local geometric structure features, PointNet++[9] groups the sampling points in the point cloud, and uses PointNet to extract local features in the local neighborhood of each sampling point, and for the density inhomogeneity of point clouds, multi-scale neighborhood retrieval and multi-resolution neighborhood retrieval are proposed. However, in the preprocess of PointNet and PointNet++, The input point cloud is divided into some $1m^2$ block with sliding window for semantic segmentation. Therefore they has poor consistency and can not have long range contextual information.

In order to extract the geometric relationship between two points in a local area, PointWeb[10] realizes feature interaction and feature optimization between local points by constructing a dense connection structure locally. Zhang et al.[11] designed a convolutional network based on shell structure. When local feature aggregation in the neighborhood of sampling points is performed, the neighborhood points are divided into different shells according to different radius ranges. Maximum pooling is used to aggregate features, and finally the features of the current center point are obtained through the features of multiple shells.

It should be pointed out that the above-mentioned point-based point cloud segmentation methods all need to perform relatively complex preprocessing on the scene point cloud. In the training phase, the scene point cloud needs to be divided into blocks([8] [9] [10] [11]), this preprocessing method inevitably destroys the consistency of the point cloud.

2.2 Projection-based method

Affected by the great success of deep neural networks in the field of 2D computer vision, a natural idea is projecting the 3D point cloud to 2D, then 2D CNN is used to extract features and segment. Finally, return 2D semantic segmentation result to point cloud.

Method based on multi-view projection([12], [13]) is sensitive to occlusion and suffers from information loss in the process of projection, failing to fully utilize the geometric structure information. Compared with the multi-view projection method, the spherical projection-based method([14], [15]) can retain more information and is more suitable for LiDAR point clouds, but it still suffers from occlusion and distortion in the projection phase.

2.3 Voxel-based method

Dense voxel-based methods ([16], [17]) voxelize the point cloud and directly apply standard 3D convolutions for point cloud semantic segmentation. Although these methods keep the original dimension of the point cloud, the voxelization step inherently introduces discretization artifacts and information loss. Usually, high resolution of voxel leads high memory and computation costs, but low resolution suffers from information loss. It is important to choose an appropriate grid resolution to have a trade-off between segmentation performance and efficiency.

Due to the sparsity of the point cloud, the number of non-zero values after voxelization only accounts for a small percentage. Therefore, it is inefficient to apply dense 3D convolution to the spatially-sparse data. To this end, sparse convolution is proposed([1], [18]), which reduces memory and computational costs by restricting the output of convolution to be only related to active point, which accelerates the computation speed by reducing the useless computation at empty voxels in point cloud. However, affected by voxel-resolution, it is not easy to perceive small-scale objects.

2.4 Hybrid method

To further leverage all available information, Hybrid methods are proposed. By fusing point clouds of different representations, such as voxel-based, projection-based and/or point-wise, Hybrid methods obtain richer features and more efficient data processing methods. 3D-MiniNet[19] extract local and global information from point cloud by a learning-based projection module and then utilize a 2D FCNN to generate high-level features to get predictions. PVCNN[20] takes point representation as 3D input data to reduce memory consumption, while convolution in voxels reduces irregular sparse data access and improves locality. SPVNAS[21] replace 3d convolution with sparse convolution, reducing unnecessary computation and improving computational efficiency, authors in SPVNAS[21] use a neural architecture search(NAS)[22] to efficiently design a NN.

The feature maps of the other three scales x_1, x_2, x_3 are passed to the feature selection module as the input of the next module.

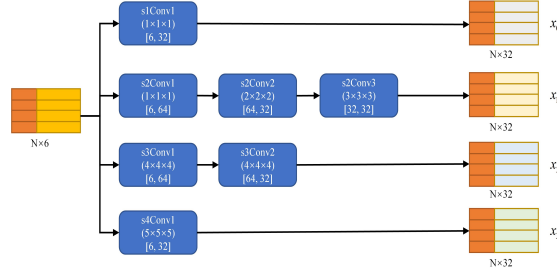


Figure 2: Multi scale feature extract module

3.3 Multi Scale Feature Fusion

For the point cloud features output from the multi-scale feature extraction module, basic fusion method is to add directly, so that the multi-scale features are regarded as the same weight, but in fact, the features of different scales should have the different influences. As shown in Figure3, inspired by SKNet[24], for the multi-scale features output by the multi-scale feature extraction module. First, the large-scale, medium-scale and small-scale features are added to obtain an intermediate feature map X , and then three different MLP s are used to perform three transformations on the intermediate feature map X :

$$\begin{aligned}
 f_1 : X &\rightarrow U_1 \in \mathbb{R}^{N \times 4} \\
 f_2 : X &\rightarrow U_2 \in \mathbb{R}^{N \times 4} \\
 f_3 : X &\rightarrow U_3 \in \mathbb{R}^{N \times 4}
 \end{aligned} \tag{1}$$

In the formula1, each transformation function f_i is a combination of convolution layer, activation function layer and BN (BatchNormalization) layer. The obtained features of different scales are spliced together and sent to the $Softmax$ activation function to obtain the score corresponding to each scale:

$$U_{cat} = cat(U_1, U_2, U_3) \tag{2}$$

$$Score = softmax(U_{cat}) \tag{3}$$

In the formula2, $U_{cat} \in \mathbb{R}^{N \times 3}$ represents the feature map after splicing the features output by formula, and in the formula 3, $Score \in \mathbb{R}^{N \times 4}$ represents the attention score of each scale. Finally, the multi-scale features are weighted and summed according to their scores to obtain the final multi-scale output. In order to retain the point-by-point scale point cloud characteristics, the input point cloud is subjected to a multi-scale addition after a Submanifold Sparse

3.4 Feature Attention Select

Convolution with a convolution kernel size of 1 and weighted addition, as the output of the multi-scale feature adaptive fusion module:

$$\text{Output} = F(x_0 + x_1 \cdot \text{Score}[:, 0] + x_2 \cdot \text{Score}[:, 1] + x_3 \cdot \text{Score}[:, 2]) \quad (4)$$

where x_0 is the output of the Submanifold Sparse Convolution with kernel size is 1, $F(\cdot)$ is the combination of sparse convolution and BatchNormalization.

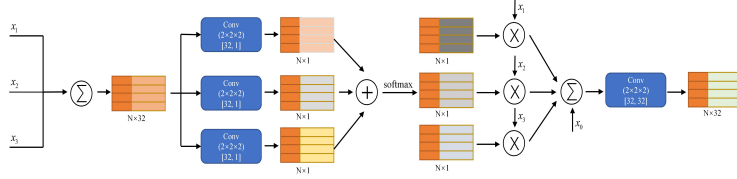


Figure 3: Multi scale feature fusion

3.4 Feature Attention Select

In the process of voxel sparse convolution, multiple convolutions are required to continuously extract deep-level features. For features in different channel, default operation is add them directly, which does not consider the importance of different channel features, will cause information lost inevitably. Inspired by SENet[25] and AF2S3Net[26], as shown in Figure4, the SE-Module is extended to 3D sparse convolution to filter the fused multi-scale features. By optimizing learning, the module can adaptively select features that contribute to the final result, while discarding those that are not important.

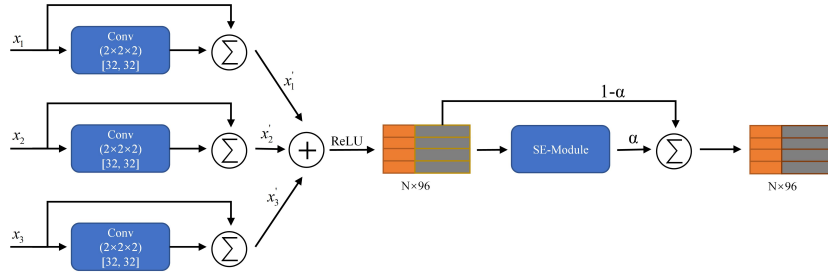


Figure 4: Feature attention select module

Figure 4 shows the feature selection module based on channel attention. For the point cloud feature maps of different scales output by the multi-scale feature extraction module, first process x_1, x_2, x_3 through the residual unit, and the output is recorded as x'_1, x'_2, x'_3 , then connect x'_1, x'_2, x'_3 and introduce nonlinearity. In the SE Module, the input point cloud feature map is passed to

global pooling operation to obtain global features:

$$x_c = \frac{1}{N} \sum_{i=1}^N x_i \quad (5)$$

where N is the voxel number, $x_i \in \mathbb{R}^{N \times C}$ donate voxel feature.

For the global features of the point cloud after the Squeeze operation, it is necessary to further obtain the feature relationship between each channel. This step is composed of two linear transformations followed by activation function:

$$s = \sigma(W_2 \delta(W_1 x_c)) \quad (6)$$

where δ is the *ReLU* activate function, σ is *Sigmoid* activate function, $W_1 \in \mathbb{R}^{\frac{C}{r} \times C}$ is the first linear transformation, compress the number of channels from C to $\frac{C}{r}$, reduce the complexity of the model, where r is the dimension reduction scale factor; $W_2 \in \mathbb{R}^{C \times \frac{C}{r}}$ is the second linear transformation which restore original number of channels.

Finally, the channel attention coefficients obtained by formula 6 are also weighted on all channels:

$$x_{output} = s_c \cdot x_c \quad (7)$$

where s_c and x_c represent the weight scores and features in different channels, s_{output} donate the output of SE module. Instead of directly passing through the weighted feature maps as output, we employed a weight factor $\alpha = 0.6$, to regularize the weighting effect.

4 Network optimization

We leveraged a linear combination of Cross-Entropy loss and Lovász-softmax loss [27] to optimize our network:

$$L(y, \hat{y}) = w_{ce} L_{ce}(y, \hat{y}) + w_{lovasz} L_{lovasz}(y, \hat{y}) \quad (8)$$

where w_{ce} and w_{lovasz} denote the weights of Cross-Entropy loss and Lovász loss respectively. They are both set as 1 in our experiments.

5 Experiments

In this section, we share the experimental results to evaluate our model. Section 5.1 briefly explains the experimental datasets. Section 5.3 contains the implementation details. Section 5.4 and Section 5.5 provides the experimental results of S3DIS [28] and SemanticKITTI [6]. Section 5.6 discuss the advantages of the proposed approach with ablation studies.

5.1 Dataset

5.1.1 S3DIS

The S3DIS dataset is a large-scale indoor point cloud scene dataset created by Stanford University in 2016. The S3DIS dataset consists of 6 different areas of three buildings used for teaching, each area contains many types of rooms, a total of 271 rooms, each point includes XYZ coordinates, RGB values and is labeled as one of 13 categories. In order to compare with previous methods, 5 regions(1, 2, 3, 4, 6) were used to train our model, and region 5 is used for the comparison of our model’s performance with previous methods.

5.1.2 SemanticKITTI

The SemanticKITTI([6]) dataset is a dataset with point-wise semantic annotations built by the University of Bonn on the basis of the KITTI dataset benchmark, showing traffic in the city center, residential areas, and highway scenes and country roads for outdoor autonomous driving scenarios. The SemanticKITTI dataset provides a total of 28 different categories, 19 of which are used for official algorithm evaluation. Due to the limited sample data, the frequency of some categories is extremely low, such as motorcyclists. The data set includes 22 sequences, with a total of 43551 frames of lidar data, among the driving sequences, 10 sequences(00 to 07, 09, 10) were used to train our model, and sequence 08 was for evaluation. The remaining sequences were used for the comparison of our model’s performance with previous methods.

5.2 Evaluation matrix

Confusion matrix is a commonly used method to express classification accuracy. As shown in the Table1, each row of values represents the predicted number of point clouds in the corresponding category after classification, and each column of values represents the actual number of a certain type of point cloud in the actual type. To evaluate the performance of the proposed method and compare with others, we leverage Intersection over Union (IoU) as our evaluation metric. IoU is the most popular metric for evaluating semantic point cloud segmentation and can be formalized as $IoU = \frac{TP}{TP+FN+FP}$, where TP is the number of true positive points, FP is the number of false positives, and FN is the number of false negatives.

Item		Ground truth	
		Positive	Negative
Prediction	Prediction	TP	FP
	Negative	FN	TN

Table 1: Confuse matrix

For the evaluation of multiple categories, the official recommendation of the SemanticKITTI dataset[6] is adopted, and mIoU(mean intersection-over-union

ratio) is used as the evaluation metric:

$$mIoU = \frac{1}{C} \sum_{c=1}^C \frac{TP_c}{TP_c + FP_c + FN_c} \quad (9)$$

5.3 Implementation details

We implement the proposed MSSNet with Pytorch. SGD optimizer with momentum is used. The voxel size is 0.05m. Also, w_{ce} and w_{lovasz} in combined loss function are both set to 1.0. Data augmentation means are consistent with the paper[7], including random scaling, rotation around the Z axis, spatial translation, and random jittering. All our experiments are conducted on two NVIDIA RTX2080Ti GPU.

On the S3DIS dataset, the hyperparameters are set as follows: batch size is 2, maximum number of iterations is 150000, initial learning rate is 0.1, learning rate adjustment strategy is Poly. On the SemanticKITTI dataset, batch size is 4, maximum number of iterations is 98500, initial learning rate is 0.24, and scheduler is cosine schedule with warmup. At the training phase, the number of input voxels in each scene is limited to 80000.

5.4 Evaluation on S3DIS

Table2 contains a quantitative result of the experiment on S3DIS[28]. From Table2, In the window category, PointNet++ is better than MinkowskiNet and the method proposed in this paper, the main reason for this phenomenon is that PointNet++ performs feature extraction pointwisely. MinkowskiNet and the method in this paper perform voxelization downsampling on the point cloud and then input it into the network, which has a lower resolution than PointNet++. Therefore, on some objects whose geometric features are not particularly obvious, the segmentation result is slightly worse than that of PointNet++. It should be noted that the preprocess of PointNet and PointNet++ is same, point cloud is cut into blocks, and then randomly select fixed points in each block as the input of network. This processing method will divide the point cloud that is originally an object into different parts as the input of the network. Although the IoU is improved, the consistency of the point cloud segmentation is poor. As shown in Figure5, different colors represent different categories, the chair in the red box is partially segmented into a table by PointNet++ wrongly. Different from the segmentation of PointNet++ and the preprocessing of randomly sampling fixed points, MinkowskiNet and the method in this paper regard the entire room as a sample and feed to the network, for some objects, long-distance context information could be better obtained, therefore, MinkowskiNet and the method in this paper are better than PointNet++ in most categories.

Figure6 visualizes some experimental results. From left to right, the RGB scene, the PointNet++ prediction result, the MinkowskiNet prediction result, the method prediction result of this paper and ground truth are displayed respectively. As can be seen from the Figure6, the prediction results of the method in this paper

5.4 Evaluation on S3DIS

Method	Ceiling	Floor	Wall	Beam	Chmn	Window	Door	Chair	Table	Bkcase	Sofa	Board	Clutter	mIoU	mAcc
PointNet	87.4	97.8	71.2	0.0	9.2	52.1	16.3	48.6	58.2	48.3	3.2	39.0	36.2	43.7	52.6
SegCloud	90.1	96.1	69.9	0.0	18.4	38.4	23.1	75.9	70.4	58.4	40.9	13.0	41.6	48.9	57.4
TangentConv	90.5	97.7	74.0	0.0	26.7	39.0	31.3	77.5	69.4	57.3	38.5	48.8	39.8	52.8	60.7
3D RNN	95.2	98.6	77.4	0.8	9.8	52.7	27.9	76.8	78.3	58.6	27.4	39.1	51.0	53.4	71.3
PointNet++	90.7	97.0	75.9	0.0	6.3	58.3	19.4	74.9	69.5	62.2	51.0	57.4	42.9	54.4	64.2
PointCNN	92.3	98.2	79.4	0.0	17.6	22.8	62.1	80.6	74.4	66.7	31.7	62.1	56.7	57.3	63.9
SuperpointGraph	89.4	96.9	78.1	0.0	42.8	48.9	61.6	84.7	75.4	69.8	52.6	2.1	52.2	58.0	66.5
PCCN	90.3	96.2	75.9	0.3	6.0	69.5	63.5	66.9	65.6	47.3	68.9	59.1	46.2	58.3	67.0
MinkowskiNet	92.6	98.2	84.3	0	37.6	51.7	73.8	90.2	73.8	69.7	63.7	66.8	55.3	65.4	72.3
MSSNet(Ours)	91.0	96.2	83.6	0	28.9	56.1	72.7	82.4	74.5	73.1	67.8	76.5	59.9	67.0	74.9

Table 2: Segmentation results of different networks on the S3DIS dataset

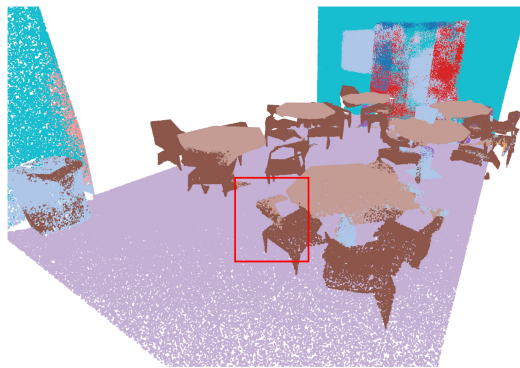


Figure 5: Error segmentation

are generally better than others, especially in some categories where the geometric information is not obvious, such as board. Compare with PointNet++, it can obtain better long-distance context information and consistency, so better semantic consistency can be obtained. Compare with MinkowskiNet, thanks to multi-scale features, the method in this paper has a significant improvement with windows, tables, bookshelves, sofas, wooden boards, miscellaneous and other categories.

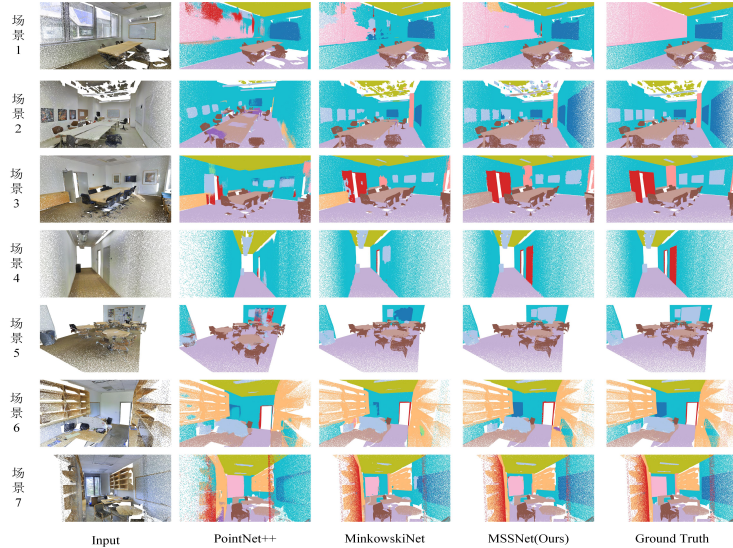


Figure 6: Visualizing the semantic segmentation results of the proposed model using Area5 in S3DIS. The first column is the RGB point cloud, the second column is the prediction of PointNet++, and the third column is the prediction of MinkowskiNet, and the 4-th column is the prediction of the proposed model, and the 5-th column is the ground truth.

5.5 Evaluation on SemanticKITTI

SemanticKITTI is an autonomous driving dataset which the point clouds are all scanned by Velodyne HLE-64E. Compare with the S3DIS dataset, the density of the SemanticKITTI dataset is more uneven.

Table3 is the comparison results of the IoU between the method proposed and MinkowskiNet and SPVCNN. It can be seen that the method proposed has the highest mIoU. Compared with MinkowskiNet, the algorithm proposed in this paper has an average cross-union ratio improvement of 4.3%. Benefiting from the multi-scale features, the algorithm proposed in this paper has a significant improvement over MinkowskiNet on some small-scale point clouds, as shown in Table3, the method proposed can obtain more accurate segmentation results. For people, bicycles, motorcycles other vehicle in the scene, the IoU of method proposed is higher than MinkowskiNet.

Table4 is the quantitative result of experiment on SemanticKITTI test data, the compared models contain point-based method, projection-based method, voxel-based method and hybrid method, the proposed method belong to voxel-based method, bold font indicates the best score in the current category, the results of MinkowskiNet and SPVCNN are the results of the paper[21]. It should be pointed out that other methods in the list may use some additional tricks to improve the IoU, while the method in this paper does not use any

5.5 Evaluation on SemanticKITTI

additional tricks. It could be found that the method in this paper has achieved leading results in mIoU and IoU of some small-scale objects (such as bicycles, motorcyclists, poles, etc.).

Method	Person	Bicycle	Bicyclist	Motorcycle	Other vertical	mIoU
MinkowskiNet	66.9	22.5	82.4	68.6	64.1	62.5
SPVCNN	69.7	35.2	82.5	64.6	64.3	63.9
MSSNet(Ours)	70.9	44.5	87.7	69.7	66.6	66.8

Table 3: Segmentation results of different methods on the SemanticKITTI validation set

Method	car	bicycle	motorcycle	truck	other-vehicle	person	bicyclist	motorcyclist	road	parking	sidewalk	other-ground	building	fence	vegetation	trunk	terrain	pole	traffic-sign	mIoU
PointNet	86.3	1.5	0.8	0.1	0.8	0.2	0.2	0.0	61.6	15.8	35.7	1.4	41.4	12.9	31.0	4.6	11.6	2.4	3.7	14.6
RandLANet	94.2	26.0	25.8	40.1	38.9	49.2	48.2	7.2	90.7	60.3	73.7	20.4	86.9	56.3	81.4	61.3	66.8	49.2	47.7	53.9
KPCovr	96.0	30.2	42.5	33.4	44.3	61.5	61.6	11.8	88.8	61.3	72.7	31.6	90.5	64.2	84.8	69.2	69.1	56.4	47.4	58.8
SequenceSegV3	92.5	38.7	36.5	29.6	31.0	45.6	46.2	20.1	91.7	63.4	74.8	26.4	89.0	59.4	82.9	58.7	65.4	49.6	58.9	55.9
RangeNet++	91.4	25.7	34.4	25.7	23.0	38.3	38.8	4.8	91.8	65.0	75.2	27.8	87.4	58.6	80.5	55.1	64.6	47.9	55.9	52.2
SalsaNet	91.9	48.3	38.6	38.9	31.9	60.2	59.0	19.4	91.7	63.7	75.8	29.1	90.2	64.2	81.8	63.6	66.5	54.3	62.1	59.5
PolarNet	95.8	40.3	30.1	22.9	28.5	43.2	40.2	5.6	90.8	61.7	74.4	21.7	90.0	61.3	84.0	65.5	67.8	51.8	57.5	54.8
MinkowskiNet	-	-	-	-	-	-	-	-	-	-	-	-	-	-	-	-	-	-	-	63.1
FusionNet	95.3	47.5	37.7	41.8	34.5	59.5	56.8	11.9	91.8	68.8	77.1	30.8	92.5	69.4	84.5	69.8	68.5	60.4	66.5	61.3
TornadoNet	94.2	55.7	48.1	40.0	38.2	63.6	60.1	34.9	89.7	66.3	74.5	28.7	91.5	65.6	85.6	67.0	71.5	58.0	65.9	63.1
AMVNet	96.2	59.9	54.2	48.8	45.7	71.0	65.7	11.0	90.1	71.0	75.8	32.4	92.4	69.1	85.6	71.7	69.6	62.7	67.2	65.3
SPVCNN	-	-	-	-	-	-	-	-	-	-	-	-	-	-	-	-	-	-	-	63.8
MSSNet(Ours)	96.8	37.8	44.5	50.3	52.1	62.8	75.2	59.8	89.6	65.2	73.1	29.5	91.0	64.7	85.3	71.1	69.6	62.7	63.8	65.8

Table 4: SemanticKITTI Test Leaderboard Results

Figure7 visualizes the semantic segmentation results of MSSNet. The test sequence is 08 sequence in SemanticKITTI[6]. As you can see, MinkowskiNet is prone to wrong segmentation for some small-scale objects, the method proposed benefits from multi-scale feature extraction and fusion, the ability to perceive small-scale objects is improved. For instance, The bicycle in the red circle in scene 1 is segmented into other categories by MinkowskiNet, but the method proposed could achieve correct semantic segmentation.

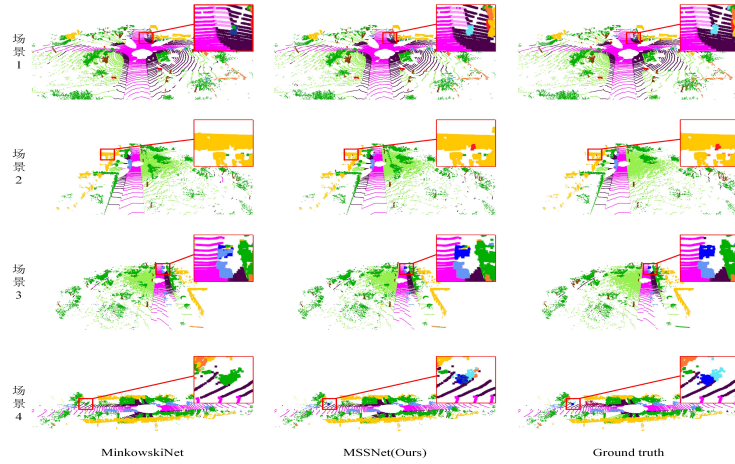


Figure 7: Visualizing the semantic segmentation results of the proposed model using 08 sequence in SemanticKITTI. The first column is the prediction of MinkowskiNet, the second column is the prediction of the proposed model, and the third column is the ground truth. We observe that the proposed model segments well at some small scale objects

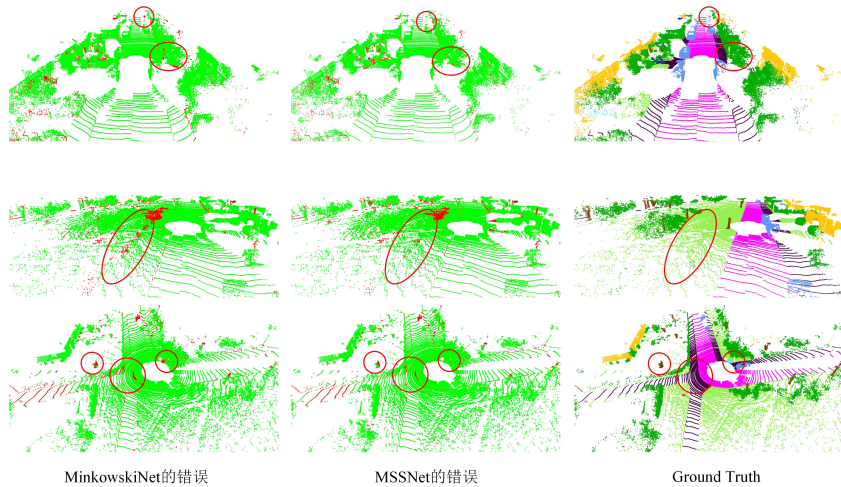


Figure 8: Visualizing the segmentation difference of the proposed model using 08 sequence in SemanticKITTI. The first column is the difference between MinkowskiNet and ground truth, the second column is the difference between MSSNet and ground truth, and the third column is the ground truth. We observe that the proposed model could reduce error segmentation

Figure8 visualizes the semantic segmentation error, red color indicates miss-

classified points, green color indicates right-classified points. Taking scene 1 as an example, in the part inside the red circle, the segmentation error area of the method proposed is significantly smaller than MinkowskiNet, which proves the effectiveness of the method in this paper.

In order to explain as much as possible that the method proposed has the property of extracting features at different scales, we visualize the concern point of convolution kernel with different scales. As shown in Figure9, different color correspond to different convolution kernel: green represents the focus of small-scale convolution kernel, dark blue represents the focus of medium-scale convolution kernel, and light blue represents the focus of large-scale convolution kernel. As we can see, The small-scale convolution kernel pays attention to some street signs, the medium-scale convolution kernel pays attention to some poles and some tree trunks, and the large-scale convolution kernel pays attention to the distant street trees and trunks. This explains that the multi-scale convolution kernels in this paper can learn features of different scales.

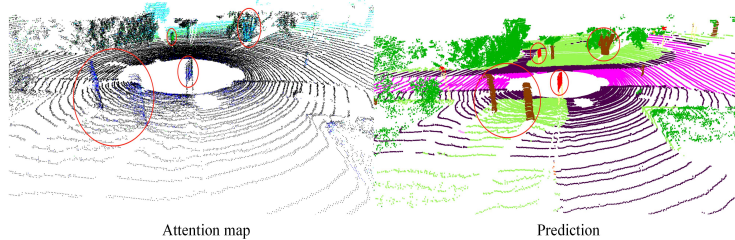


Figure 9: Attention map on SemanticKITTI sequence 08

5.6 Ablation studies

In order to verify the functions of different modules of the algorithm in this chapter, ablation experiments are designed on the S3DIS dataset to analyze the effects of multi-scale feature extraction and multi-scale feature fusion. The basic network of this paper is the U-shaped network after removing the multi-scale feature module and the channel attention-based feature selection module. First train base network using the cross-entropy loss function; Secondly, let the multi-scale feature module only output the fused multi-scale features without feature selection; The features of different scales are not fused, and are directly input into the feature selection module based on channel attention, and the network structure after only adding the feature selection module is obtained. On top of the structure of the basic network, a multi-scale feature module and a channel attention-based feature selection module are both added. Finally, the lovász-softmax loss function[27] is added to the loss function, and the obtained results are shown in Table5.

Observing Table5, we can see that after adding the multi-scale feature module,

5.7 Evaluation by distance

the mIoU value is increased from 64.33% of the basic network to 66.35%, which shows the importance of multi-scale features. The feature output of three different scales before the fusion is used as the input of the multi-scale feature selection module, the mIoU of the network is 64.50%, compared with the basic network, there is a certain improvement, but the improvement is limited, mainly because the multi-scale features after fusion are not added. If both modules are turned on and the network training is supervised by the cross-entropy loss function, mIoU obtained from the test is 66.47%. Adding the lovász-softmax loss function[27] to the network optimization process, the final average intersection-over-union ratio mIoU is 67.03%. Ablation experiments show that the multi-scale feature extraction and fusion module and the channel attention-based feature selection module proposed in this paper can improve the multi-scale feature representation ability of the network to improve the segmentation accuracy of the network.

Module	MSFM	FSM	lovász-softmax	mIoU(%)
Baseline				64.33
	✓			66.35
Proposed		✓		64.50
	✓	✓		66.47
	✓	✓	✓	67.03

Table 5: Ablation study of the proposed method vs baseline evaluated on S3DIS validation dataset

5.7 Evaluation by distance

In order to verify the robustness of the point cloud scene segmentation method proposed, experiments are carried out on SemanticKITTI. In order to show the improvements, we compare MinkowskiNet and SPVCNN on the SemanticKITTI validation set (seq 8). Fig10 illustrates the mIoU of MinkowskiNet, SPVCNN and MSSNet(proposed) with different distance. The results of all the methods get worse by increasing the distance due to the fact that point clouds generated by LiDAR are relatively sparse, specially at large distances. In different regions, the mIoU value of the algorithm proposed is always higher than SPVCNN and MinkowskiNet, of which MinkowskiNet is the lowest, this is because the SPVCNN utilizes fine-grained point features, so higher mIoU can be obtained at longer distances. The method proposed could capture multi-scale features, therefore, it has better segmentation results in each distance range, it is proved that the method proposed has good robustness.

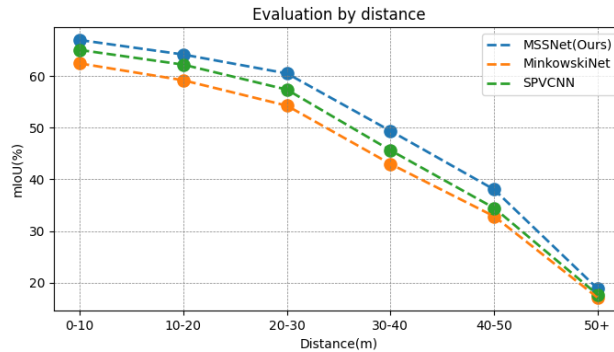


Figure 10: mIoU vs Distance

6 Conclusion

In this paper, we proposed MSSNet the multi scale based sparse convolution model for point cloud semantic segmentation. The multi-scale feature extraction module proposed in this paper uses convolution kernels with different sizes to extract features with different scales. In order to fuse point cloud features of different scales, this paper proposed a multi-scale feature fusion module based on attention mechanism. Aiming at the problem that multi-scale features introduce redundant features, this paper proposed a feature selection module based on channel attention to filter high-dimensional features. Finally, we conducted the extensive evaluation and discussion of the proposed model on S3DIS and SemanticKITTI dataset, which demonstrate the effectiveness and superiority of proposed method.

Acknowledgments

References

- [1] Yan Yan, Yuxing Mao, and Bo Li. Second: Sparsely embedded convolutional detection. *Sensors*, 18(10):3337, 2018.
- [2] Shaoshuai Shi, Chaoxu Guo, Li Jiang, Zhe Wang, Jianping Shi, Xiaogang Wang, and Hongsheng Li. Pv-rcnn: Point-voxel feature set abstraction for 3d object detection. In *Proceedings of the IEEE/CVF Conference on Computer Vision and Pattern Recognition*, pages 10529–10538, 2020.
- [3] Zhoutao Wang, Qian Xie, Mingqiang Wei, Kun Long, and Jun Wang. Multi-feature fusion votenet for 3d object detection. *ACM Transactions on Multimedia Computing, Communications, and Applications (TOMM)*, 18(1):1–17, 2022.

REFERENCES

- [4] Lue Fan, Ziqi Pang, Tianyuan Zhang, Yu-Xiong Wang, Hang Zhao, Feng Wang, Naiyan Wang, and Zhaoxiang Zhang. Embracing single stride 3d object detector with sparse transformer. *arXiv preprint arXiv:2112.06375*, 2021.
- [5] Alex H Lang, Sourabh Vora, Holger Caesar, Lubing Zhou, Jiong Yang, and Oscar Beijbom. Pointpillars: Fast encoders for object detection from point clouds. In *Proceedings of the IEEE/CVF Conference on Computer Vision and Pattern Recognition*, pages 12697–12705, 2019.
- [6] Jens Behley, Martin Garbade, Andres Milioto, Jan Quenzel, Sven Behnke, Cyrill Stachniss, and Jurgen Gall. Semantickitti: A dataset for semantic scene understanding of lidar sequences. In *Proceedings of the IEEE/CVF International Conference on Computer Vision*, pages 9297–9307, 2019.
- [7] Christopher Choy, JunYoung Gwak, and Silvio Savarese. 4d spatio-temporal convnets: Minkowski convolutional neural networks. In *Proceedings of the IEEE/CVF Conference on Computer Vision and Pattern Recognition*, pages 3075–3084, 2019.
- [8] Charles R Qi, Hao Su, Kaichun Mo, and Leonidas J Guibas. Pointnet: Deep learning on point sets for 3d classification and segmentation. In *Proceedings of the IEEE conference on computer vision and pattern recognition*, pages 652–660, 2017.
- [9] Charles Ruizhongtai Qi, Li Yi, Hao Su, and Leonidas J Guibas. Pointnet++: Deep hierarchical feature learning on point sets in a metric space. *Advances in neural information processing systems*, 30, 2017.
- [10] Hengshuang Zhao, Li Jiang, Chi-Wing Fu, and Jiaya Jia. Pointweb: Enhancing local neighborhood features for point cloud processing. In *Proceedings of the IEEE/CVF conference on computer vision and pattern recognition*, pages 5565–5573, 2019.
- [11] Zhiyuan Zhang, Binh-Son Hua, and Sai-Kit Yeung. Shellnet: Efficient point cloud convolutional neural networks using concentric shells statistics. In *Proceedings of the IEEE/CVF international conference on computer vision*, pages 1607–1616, 2019.
- [12] Maxim Tatarchenko, Jaesik Park, Vladlen Koltun, and Qian-Yi Zhou. Tangent convolutions for dense prediction in 3d. In *Proceedings of the IEEE Conference on Computer Vision and Pattern Recognition*, pages 3887–3896, 2018.
- [13] Felix Järemo Lawin, Martin Danelljan, Patrik Tosteberg, Goutam Bhat, Fahad Shahbaz Khan, and Michael Felsberg. Deep projective 3d semantic segmentation. In *International Conference on Computer Analysis of Images and Patterns*, pages 95–107. Springer, 2017.

REFERENCES

- [14] Andres Milioto, Ignacio Vizzo, Jens Behley, and Cyrill Stachniss. Rangenet++: Fast and accurate lidar semantic segmentation. In *2019 IEEE/RSJ International Conference on Intelligent Robots and Systems (IROS)*, pages 4213–4220. IEEE, 2019.
- [15] Bichen Wu, Xuanyu Zhou, Sicheng Zhao, Xiangyu Yue, and Kurt Keutzer. Squeezesegv2: Improved model structure and unsupervised domain adaptation for road-object segmentation from a lidar point cloud. In *2019 International Conference on Robotics and Automation (ICRA)*, pages 4376–4382. IEEE, 2019.
- [16] Lyne Tchapmi, Christopher Choy, Iro Armeni, JunYoung Gwak, and Silvio Savarese. Segcloud: Semantic segmentation of 3d point clouds. In *2017 international conference on 3D vision (3DV)*, pages 537–547. IEEE, 2017.
- [17] Dario Reithage, Johanna Wald, Jurgen Sturm, Nassir Navab, and Federico Tombari. Fully-convolutional point networks for large-scale point clouds. In *Proceedings of the European Conference on Computer Vision (ECCV)*, pages 596–611, 2018.
- [18] Benjamin Graham, Martin Engelcke, and Laurens Van Der Maaten. 3d semantic segmentation with submanifold sparse convolutional networks. In *Proceedings of the IEEE conference on computer vision and pattern recognition*, pages 9224–9232, 2018.
- [19] Inigo Alonso, Luis Riazuelo, Luis Montesano, and Ana C Murillo. 3d-mininet: Learning a 2d representation from point clouds for fast and efficient 3d lidar semantic segmentation. *IEEE Robotics and Automation Letters*, 5(4):5432–5439, 2020.
- [20] Zhijian Liu, Haotian Tang, Yujun Lin, and Song Han. Point-voxel cnn for efficient 3d deep learning. In *Advances in Neural Information Processing Systems*, 2019.
- [21] Haotian Tang, Zhijian Liu, Shengyu Zhao, Yujun Lin, Ji Lin, Hanrui Wang, and Song Han. Searching efficient 3d architectures with sparse point-voxel convolution. In *European conference on computer vision*, pages 685–702. Springer, 2020.
- [22] Chenxi Liu, Barret Zoph, Maxim Neumann, Jonathon Shlens, Wei Hua, Li-Jia Li, Li Fei-Fei, Alan Yuille, Jonathan Huang, and Kevin Murphy. Progressive neural architecture search. In *Proceedings of the European conference on computer vision (ECCV)*, pages 19–34, 2018.
- [23] Hao Fang and Florent Lafarge. Pyramid scene parsing network in 3d: Improving semantic segmentation of point clouds with multi-scale contextual information. *Isprs journal of photogrammetry and remote sensing*, 154:246–258, 2019.

REFERENCES

- [24] Xiang Li, Wenhai Wang, Xiaolin Hu, and Jian Yang. Selective kernel networks. In *Proceedings of the IEEE/CVF Conference on Computer Vision and Pattern Recognition*, pages 510–519, 2019.
- [25] Jie Hu, Li Shen, and Gang Sun. Squeeze-and-excitation networks. In *Proceedings of the IEEE conference on computer vision and pattern recognition*, pages 7132–7141, 2018.
- [26] Ran Cheng, Ryan Razani, Ehsan Taghavi, Enxu Li, and Bingbing Liu. 2-s3net: Attentive feature fusion with adaptive feature selection for sparse semantic segmentation network. In *Proceedings of the IEEE/CVF conference on computer vision and pattern recognition*, pages 12547–12556, 2021.
- [27] Maxim Berman, Amal Rannen Triki, and Matthew B Blaschko. The lovász-softmax loss: A tractable surrogate for the optimization of the intersection-over-union measure in neural networks. In *Proceedings of the IEEE conference on computer vision and pattern recognition*, pages 4413–4421, 2018.
- [28] Iro Armeni, Ozan Sener, Amir R Zamir, Helen Jiang, Ioannis Brilakis, Martin Fischer, and Silvio Savarese. 3d semantic parsing of large-scale indoor spaces. In *Proceedings of the IEEE conference on computer vision and pattern recognition*, pages 1534–1543, 2016.